

Effect of Selected Natural compounds on self-assembly of proteins

Traditionally, natural compounds have been known for their medicinal values to treat a number of health complications. A range of natural compounds, including curcumin, eugenol, capsaicin and ajmalicine, has been already reported in literature for their specific medicinal properties such as anti-cancerous (O'Dwyer, Leyland-Jones et al. 1985)], anti-hypertensive (Noble 1990)] and anti-inflammatory effects. Therefore, understanding the mechanism of interactions between biomolecules and natural compounds become very important.

In this chapter, effect of both eugenol and capsaicin was extensively studied on the aggregation process of selected proteins. Eugenol is a versatile natural compound, having several medicinal applications (Prasad, Ansari et al. 2010) which include its anti-inflammatory, anti-tumorigenic and anti-oxidant properties (Mnafgui, Hajji et al. 2015). It has been reported that eugenol is capable to interact with different proteins and it is also efficient enough to influence their functional properties (Fujisawa and Masuhara 1981; Bi, Yan et al. 2012; Varman and Singh 2012). Hence, in this section of the chapter, properties of eugenol were studied on amyloid formation of globular proteins. Here, insulin and serum albumin were considered as convenient model systems to study amyloid formation of globular proteins.

In the next section of this chapter, effect of capsaicin was examined on the biophysical properties of both molecular and fibrillar forms of collagen. Capsaicin is mainly used as an analgesic agent in many pain relieving medicines, gels and sprays. Capsaicin is known to penetrate the skin by crossing the extra cellular matrix (ECM) (Kielty and Grant 2003). Since, collagen is the major component of the extra cellular matrix it is important to understand collagen-capsaicin interactions. Experimental data on collagen-capsaicin relationship is scarce in literature. Here, type I collagen was considered as a convenient model structural protein to study collagen fibril formation in the presence of capsaicin. In addition to the experimental studies, different computational methods were also used to further understand the molecular interactions between collagen and capsaicin.

4.1 ANTIAMYLOIDOGENIC ACTIVITY OF EUGENOL

Eugenol (4-Alkyl-2-methoxyphenol; Figure 4.7b) is a phenolic compound which belongs to a class of phenylpropanoid compounds. It is mostly found in the essential oils that are extracted from clove, basil, cinnamon and bay-leaf (Fujisawa and Masuhara 1981; Cho, Kim et al. 2008). Eugenol is reported for its versatile properties, like anti-oxidant, anti-inflammatory and anti-tumorigenic activities. Recently anti-asthmatic property of eugenol was also reported in a mouse model (Pan and Dong 2015). In another recent investigation, it has been reported that eugenol can efficiently inhibit the key enzymes related to diabetes and hypertension (Mnafgui, Hajji et al. 2015), both in *in vivo* and *in vitro* model systems. Furthermore, eugenol is known to suppresses the activity of Cl⁻ Channel TMEM16A (Yao, Namkung et al. 2012). Some other studies on cell models have proved that eugenol can protect PC12 cells from toxic amyloids (Irie and Keung 2003; Liang, Cheng et al. 2015). Eugenol is also known to suppress the occurrence of dopamine depression and lipid peroxidation inductivity, which are directly linked to Parkinson's disease (Kabuto, Tada et al. 2007). Considering such neuroprotective

nature of eugenol against toxic amyloids, elucidation of the effect of eugenol on amyloid formation of proteins becomes very important. The formation of amyloids is known to be associated with the severe amyloid-linked diseases (Chiti and Dobson 2006; Greenwald and Riek 2010). Therefore, targeting the onset of amyloid formation can be considered as one of the critical strategies to prevent amyloid linked diseases and its associated medical severities.

Here in this current work, the temperature induced amyloid formation of two selected globular proteins, insulin and serum albumin (BSA), was demonstrated in the presence and in the absence of eugenol. These globular proteins are also known to form amyloid fibrils under *in vitro* conditions (Holm, Jespersen et al. 2007; Dubey, Anand et al. 2014; Gong, He et al. 2014; Jayamani and Shanmugam 2014). Hence, these two proteins were selected as convenient model systems to elucidate the anti-amyloid activity of eugenol. The main focus of this work was to investigate the inhibitory effect of eugenol on both spontaneous and seed-induced amyloid formation of proteins, under *in vitro* conditions.

4.1.1 Eugenol Prevents Amyloid Formation of Globular Proteins

Amyloid formation of both insulin and serum albumin was initiated by incubating the protein monomer samples in PBS at an elevated temperature close to their T_m values (Dubey, Anand et al. 2014). Aggregation kinetics of proteins was monitored by measuring the ThT readings of the samples at different time points. While monitoring the ThT signals of the protein samples it was observed that in the presence of eugenol formation of amyloid fibrils was substantially low. This inhibition effect of eugenol was observed in both the proteins, insulin as well as for BSA (Figure 4.1a and 4.1c). Since eugenol stocks were prepared in ethanol (see Annexure A) and ethanol is known to interfere with some proteins during their aggregation (Goda, Takano et al. 2000), it is important to study the effect of ethanol on aggregation kinetics of proteins. To address this issue experiments were carried out to examine the effect of ethanol and the obtained data was clearly indicating that the amount of ethanol added to the samples was not having any effect on protein aggregation (Figure 4.2a). Hence, in the current study, the decrease in Thioflavin T signals signifies that the inhibition of the amyloid formation was due to the presence of eugenol. The nature of the aggregation curves obtained from Thioflavin T assays indicated a decrease in the extent of amyloid formation in the presence of eugenol. Such results suggest that the eugenol molecule is capable of interfering with both initiation of aggregation and the elongation process of fibril formation (growth phase). To shed light on these critical questions, AFM images of mature insulin fibrils (Figure 4.3a) were obtained from the inhibited aggregation reactions and the results showed typical amyloid morphology as seen for insulin (Siposova, Kubovcikova et al. 2012). However, a large population of oligomeric species was observed in the same sample (Figure 4.3b). These spheroidal oligomers have also been observed to occur during the progression of protein amyloid formation such as in the case of insulin (Liu, Zhang et al. 2012) and α -synuclein (Apetri, Maiti et al. 2006). Similar results were obtained in case of BSA, when AFM images of samples taken from an inhibited aggregation reaction of BSA in the presence of eugenol (Figure 4.3c). The oligomeric species of BSA displayed a proto-fibrillar appearance (Figure 4.3d) rather than spheroidal structures as seen for insulin. Mature fibrils taken from both inhibited and uninhibited reactions of proteins look almost similar for both insulin and BSA (Figure 4.3a, 4.3c and 4.4a). Considering the suppression of Thioflavin T signals and the occurrence of large population of oligomers in the inhibited aggregation reactions of proteins, it seems that eugenol has the potential to restrict such low molecular weight assembled structure to grow into mature fibrils.

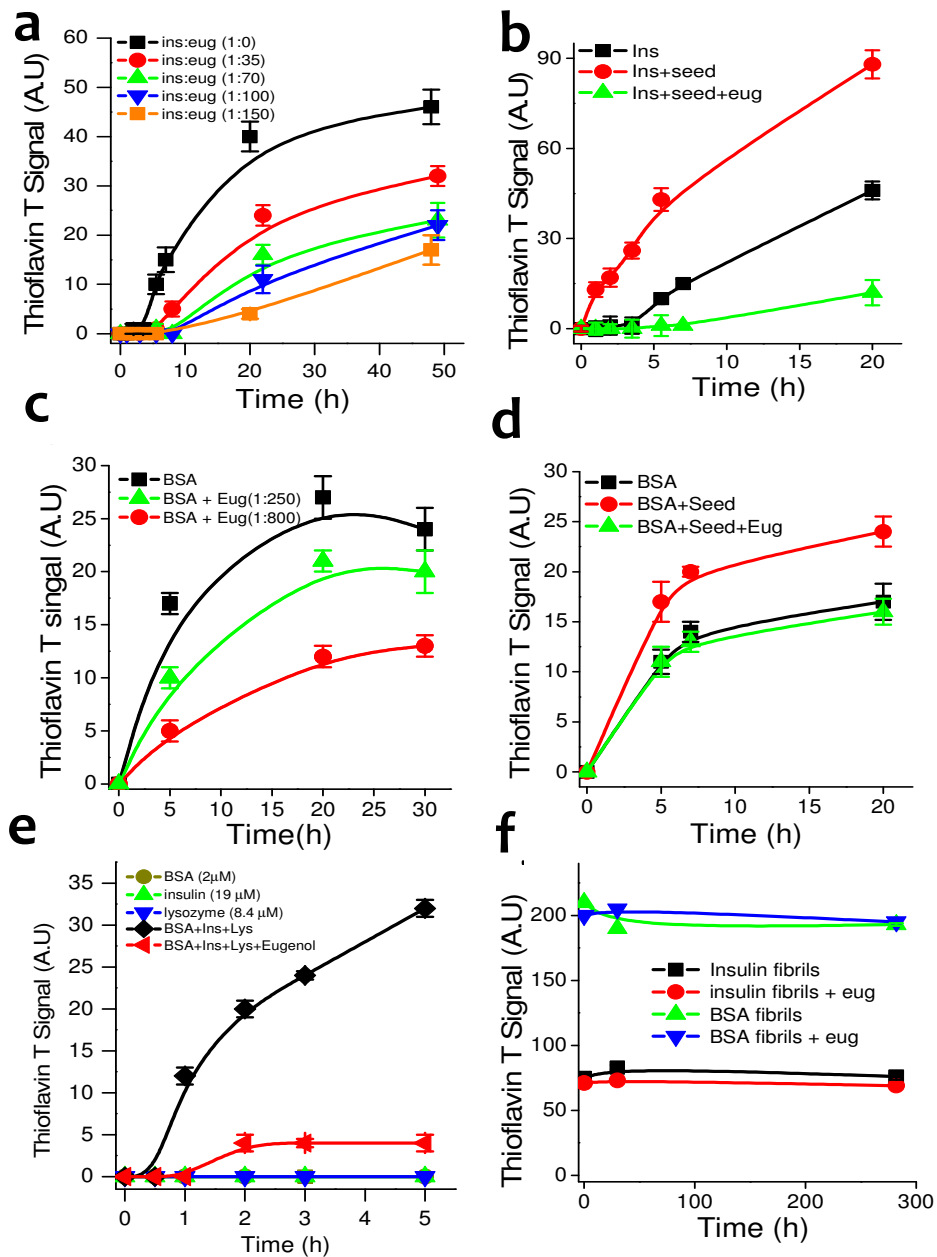


Figure 4.1: Inhibition of insulin and BSA amyloid formation in the presence of eugenol. (a) Effect of eugenol on spontaneous aggregation of insulin (~43 μM) at different molar ratios; 1:0 (■), 1:35 (●), 1:70 (▲), 1:100 (▼) and 1:150 (■). (b) Seed-induced aggregation of insulin (at ~43 μM): Insulin alone (■), insulin + seed (●); insulin + seed + eugenol at 1:100 molar ratio of protein:inhibitor (▲). (c) Effect of eugenol on spontaneous aggregation of BSA (at ~6.5 μM): BSA only (■); BSA+eugenol at 1:250 molar ratio of protein:inhibitor (▲); BSA+eugenol at 1:800 molar ratio of protein:inhibitor (●). (d) Seed induced aggregation of BSA (~3 μM); BSA only (■), BSA + seeds (●), and BSA + seeds + eugenol (1:400 molar ratio) (▲). (e) Effect of eugenol on coaggregation of BSA, insulin and lysozyme: ~2 μM BSA (●), ~19 μM Insulin (▲), ~8.4 μM lysozyme (▼), [2 μM BSA+ 19 μM Insulin+ 8.4 μM lysozyme] (◆), [2 μM BSA+ 19 μM Insulin+ 8.4 μM lysozyme + 3 mM eugenol] (▲). (f) Effect of eugenol on the disassembly process of matured amyloid fibrils of insulin and BSA; Insulin amyloids (■), insulin amyloids + eugenol (1:100 molar ratio of protein:inhibitor) (●), BSA amyloids (▲), BSA amyloids + eugenol (1:400 molar ratio of protein:inhibitor) (▼). Until ~300 hr of observation, no indication of dissociation of amyloid fibrils was observed. Seed implies 15% (w/w) preformed mature fibrils of the protein sample.

To further confirm this interpretation, the effect of eugenol was examined on seed-induced aggregation of proteins. The data obtained after adding ~15% (w/w) preformed fibrils to both insulin and BSA showed aggressive aggregation profiles (Figure 4.1b and 4.1d). However, inhibition of seed-induced aggregation was observed when both insulin and BSA samples were incubated with eugenol treated seeds (Figure 4.1b and 4.1d). This suggests that the eugenol molecule is either capable of binding to the protein monomers or it may perhaps interact with the preformed amyloid fibrils or protofibrils, apparently blocking the growth phase of the aggregation reaction. The affinity of eugenol towards the amyloid fibrils was further confirmed by conducting sedimentation assays (see Annexure A). Results suggest a dose dependent affinity of eugenol molecule for mature amyloid fibrils of both BSA and insulin (Figure 4.6d).

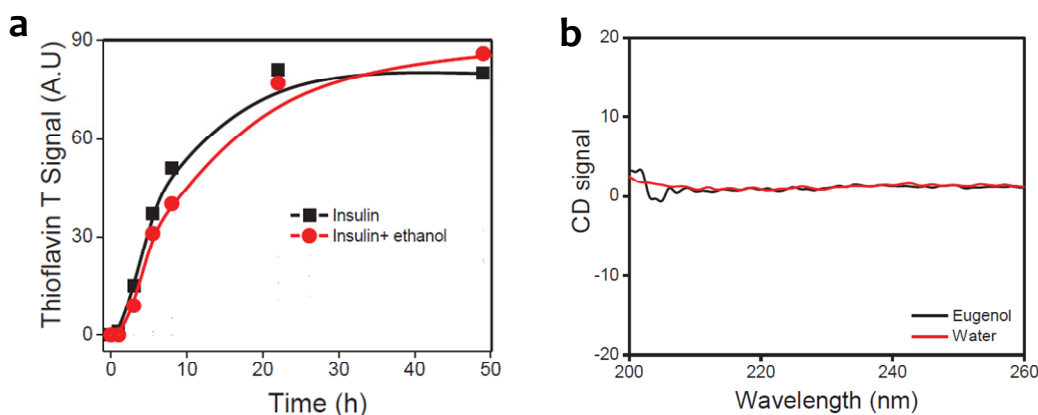


Figure 4.2 : Control experiments for aggregation and CD experiments. (a) Kinetics of amyloid formation of insulin measured through ThT assay. (b) CD spectra of eugenol at ~0.4 mM (—) and water (—).

4.1.2 Effect of Eugenol on Coaggregation of Proteins

Recently, the occurrence of rapid coaggregation of globular proteins into amyloid fibrils was reported (Dubey, Anand et al. 2014). This investigation was conducted under *in vitro* conditions, where the aggregation kinetics of coaggregated samples was observed much faster than the kinetics observed for individual aggregation reactions. Here, the effect of eugenol was also tested on the coaggregation process of three selected globular proteins (BSA, insulin and lysozyme). Results clearly represents the rapid coaggregation (Figure 4.1e, ◆) when a mixture of BSA, insulin and lysozyme was kept together in aggregating conditions. Whereas no aggregation was observed for individual protein samples (Figure 4.1e, ●▲▼). However, such coaggregation process is substantially suppressed in the presence of eugenol (Figure 4.1e, ◀). The ability of eugenol to inhibit both individual aggregation reactions and coaggregation reactions clearly suggests that the inhibition mechanism may involve common driving forces irrespective of the sequence identities of the aggregating species. To further understand the eugenol-amyloid interaction, disassembly studies were conducted on matured amyloid fibrils of proteins in presence of eugenol. Notably, no effect of eugenol was observed on the dissociation of amyloid fibrils as shown in Figure 4.1f.

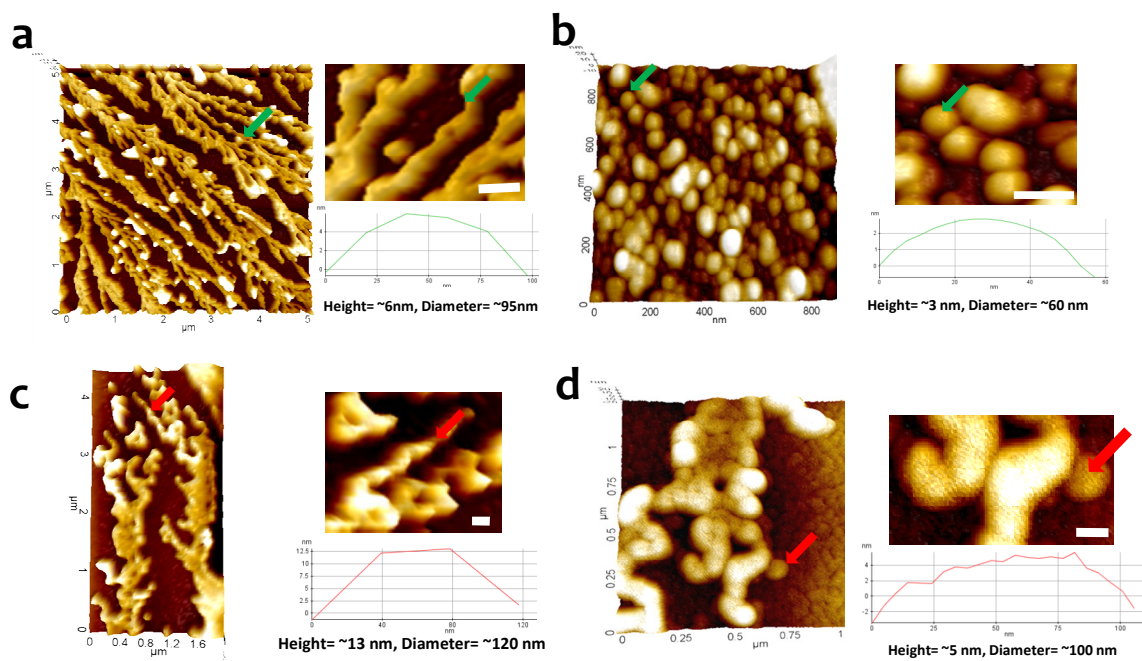


Figure 4.3 : AFM images of Insulin and BSA aggregates formed in presence of eugenol. (a) Mature Insulin amyloids after 72 h incubation. (b) Spheroidal oligomers of insulin observed after ~72 h incubating sample. (c) Mature amyloids of BSA, after ~72 H incubation. (d) Protofibrillar assemblies obtained in BSA sample incubated for ~72 h. Scale Bar, ~100 nm.

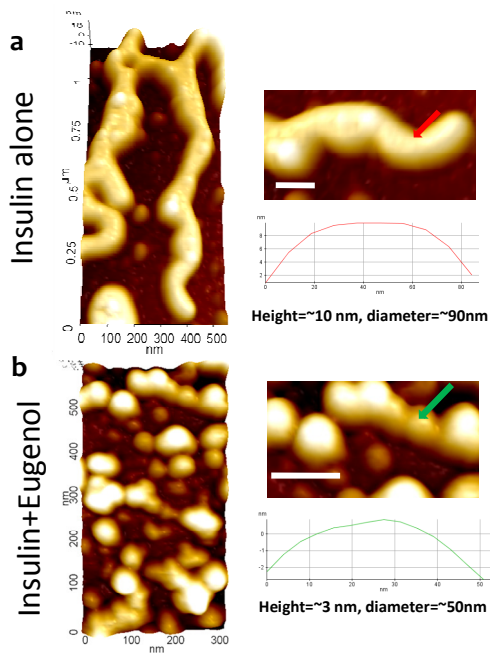


Figure 4.4 : AFM images from 5 hours incubated sample of Insulin aggregates, formed in the presence and in the absence of eugenol. (a) Insulin aggregates in the absence of eugenol. (b) Oligomers turning to protofibrils in the presence of eugenol. Scale bar, ~100 nm.

4.1.3 CD-Spectroscopy Studies

It is important to look at the structural changes taking place in protein molecules during aggregation process. CD spectroscopy was employed to study the conformational changes in proteins. First, CD spectra of eugenol alone were recorded to confirm that eugenol itself was not causing any interference with CD signals (Figure 4.2b). Further, CD spectra from both inhibited and uninhibited reactions of insulin and BSA were collected at different time points during their aggregation reaction (Figure 4.5a and 4.5c). In Figure 4.5a and 4.5c CD curves of both inhibited and uninhibited reactions of BSA and insulin were shown when recorded at 0 and 90 h. The molecular conformations of BSA (Figure 4.5a, — and — curves) and insulin (Figure 4.5c, — and — curves) remain unchanged in the presence of eugenol at 0 h. However, during aggregation, it appears that the process of conversion of native protein molecules into β -sheet assembled species is delayed in the presence of eugenol (blue and red curves of (Figure 4.5a, and 4.5c). Thioflavin T signals were also recorded for the same CD samples and the data are shown in the insets of Figure 4.5a and 4.5c. Thioflavin T data strongly support the interpretation of CD results. To further confirm the retention of native state of proteins in the presence of eugenol, native gel-electrophoresis experiments were carried out. The obtained result supports this hypothesis that eugenol helps proteins to retain their native structures during the onset of aggregation process (Figure 4.5b).

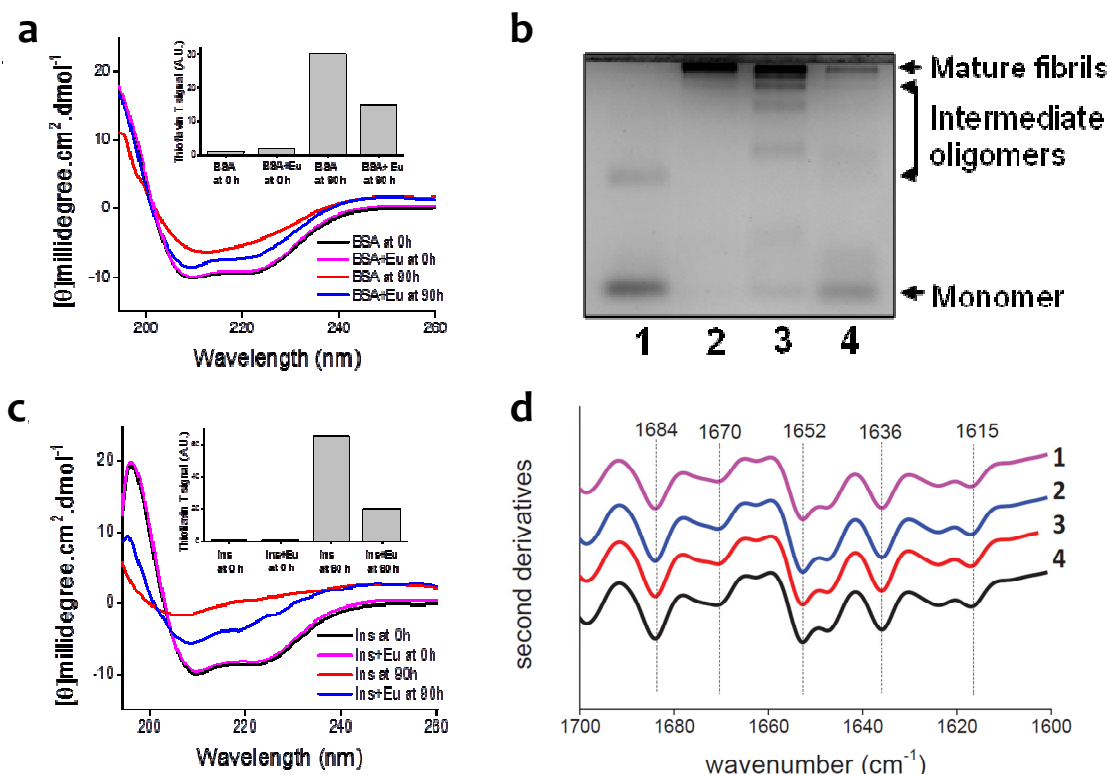


Figure 4.5 : Structural studies on eugenol-protein interaction. (a) CD spectra of BSA undergoing aggregation in the presence and in the absence of eugenol (molar ratio of protein:ligand was 1:400): BSA only at 0 h (—); BSA + eugenol at 0 h (—); BSA only at 90 h (—); BSA + eugenol at 90 h (—). (b) Native gel-electrophoresis of the BSA ($\sim 5\mu\text{M}$) undergoing amyloid formation in the presence and absence of eugenol (at $\sim 3\text{mM}$): (1) soluble BSA; (2) mature BSA aggregates; (3) Sample taken from an aggregation reaction of BSA in the absence of eugenol at 5 h; (4) Sample taken from an aggregation reaction of BSA in the presence of eugenol at 5h. (c) CD spectra of insulin undergoing aggregation in the presence and in the absence of eugenol (molar ratio of protein:ligand was 1:100): insulin only at 0 h (—); insulin + eugenol at 0 h (—); insulin only at 90 h (—); insulin + eugenol at 90 h (—). Insets shown in the panel A and panel B show Thioflavin data for the respective CD samples. (d) ATR FTIR second derivative spectra of final aggregates: 1) insulin aggregates in eugenol (molar ratio of protein: ligand is 1:100); 2) insulin aggregates in the absence

of eugenol; 3) BSA aggregates in eugenol (molar ratio of protein: ligand is 1:400); 4) BSA aggregates in the absence of eugenol.

4.1.4 Fourier Transform Infrared Spectroscopy (FTIR) Studies of Protein Aggregates

In order to examine the effect of eugenol on the structural properties of amyloid fibrils, FTIR spectroscopy was employed to analyze BSA and insulin amyloid fibrils formed in the presence and in the absence of eugenol. Obtained FTIR data, as shown in Figure 4.4d, represents the second derivative spectra of the aggregate samples after smoothening and baseline correction in the amide I region (1700 cm^{-1} to 1600 cm^{-1}). The signatures of all the FTIR curves look identical to each other (Figure 4.4d). Several characteristic peaks at 1615 cm^{-1} , 1636 cm^{-1} , 1652 cm^{-1} , 1670 cm^{-1} and 1684 cm^{-1} were also observed for all the obtained FTIR curves. The peak at 1615 cm^{-1} suggests the occurrence of intermolecular β -sheets and both peaks at 1670 cm^{-1} and 1684 cm^{-1} indicate the presence of β -turns. Information obtained from FTIR data on the structural properties reveals that the fibrils generated from both inhibited and uninhibited reactions have similar secondary structures. It is possible that eugenol suppresses the aggregation process without affecting the aggregation pathway.

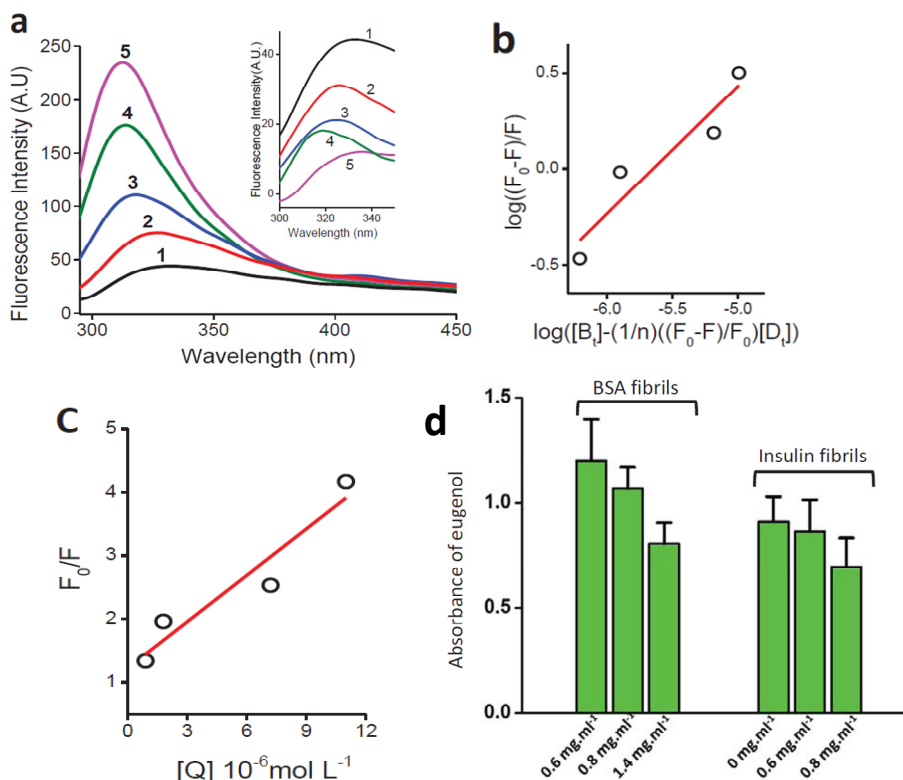


Figure 4.6: (a) Fluorescence spectra of eugenol sample (at 1.65 μM) with increasing concentrations of insulin. Excitation wavelength was 262 nm. Concentrations of insulin were: 1) 0 μM ; 2) 1 μM ; 3) 2 μM ; 4) 7 μM ; 5) 11 μM . The inset shows the baseline corrected emission curves of eugenol. (b) The curve of $\log((F_0 - F)/F)$ versus $\log([B] - (1/n)[D]((F_0 - F)/F_0)[D])$ for eugenol binding with insulin. (c) Stern-Volmer plot of eugenol and insulin. All the fluorescence measurements were carried out at room temperature. (d) Sedimentation assay for determining the affinity of eugenol to amyloid fibril of BSA and Insulin.

4.1.5 Intrinsic Fluorescence Studies of Eugenol-Insulin Interaction

Next, fluorescence technique was used to gain further information on insulin-eugenol interactions. Using established protocols (Chamani, Tafrishi et al. 2010; Sarzehi and Chamani 2010), eugenol quenching was measured in the presence of insulin and the obtained data were used to calculate Stern-Volmer constant (K_{sv}), quenching rate constant (K_q), binding constant (K_a) and binding site (n) parameters. Eugenol emits fluorescence at 325 nm when it is excited at 262

nm (Bi, Yan et al. 2012). The fluorescence spectra of eugenol in the presence of different concentrations of insulin were shown in Figure 4.6a. The inset of Figure 4.6a shows the baseline corrected quenching data of eugenol in the presence of insulin. These data clearly reveal that fluorescence emission of eugenol was significantly quenched by insulin, and there was a gradual decrease in the eugenol fluorescence by increasing insulin concentration (inset Figure 4.6a). To calculate the magnitude and the nature of the quenching phenomenon from this study, the fluorescence emission spectra were analyzed using Stern-Volmer equation (Lakowicz and Weber 1973; Chinnathambi, Velmurugan et al. 2014) and the obtained plot was shown in Figure 4.6c. The values of K_{sv} and k_q were found to be $2.5 \times 10^5 \text{ L mol}^{-1}$ and $2.5 \times 10^{13} \text{ L mol}^{-1} \text{ s}^{-1}$ respectively. Since the value of k_q is greater than $2.0 \times 10^{10} \text{ L mol}^{-1} \text{ s}^{-1}$, the quenching process of eugenol by insulin was predicted to be static. Further the binding constant (K_a) and binding site (n) parameters were calculated by using reported analysis equations (Sun, Zhang et al. 2011; Bi, Yan et al. 2012). The value of K_a was observed to be $5.8 \times 10^3 \text{ L mol}^{-1}$ and the binding site parameter (n) was observed to be ~ 1.5 , suggesting a single binding site.

4.1.6 Molecular Docking of Eugenol with Proteins

Molecular docking studies were performed to understand the affinity of eugenol for native protein structures of insulin and BSA. Blind docking studies were carried out to understand the molecular interactions between eugenol and these proteins and obtained data were shown in Figure 4.7a and 4.7b. The value of CDocker energy obtained for insulin-eugenol interaction was found to be $-4.1 \text{ kcal mol}^{-1}$ and the value of corresponding interaction energy was $-13.5 \text{ kcal mol}^{-1}$. The structure of insulin-eugenol complex was shown in Figure 4.7b and such complex predicts four hydrogen bonds and one pi-alkyl interaction (Table 4.2). Similarly for BSA-eugenol interaction, the value of CDocker energy was found to be $-13.9 \text{ kcal mol}^{-1}$, and the corresponding interaction energy was observed to be $-28.5 \text{ kcal mol}^{-1}$. Figure 4.7a summarizes the interactions between BSA and eugenol and it displays one hydrogen bond, three alkyl interactions and three pi-alkyl interactions (Table 4.1). The values of CDocker energies obtained from insulin-eugenol and BSA-eugenol docking studies clearly indicate the formation of stable protein-eugenol complexes. The value of K_a obtained from intrinsic fluorescence quenching studies for eugenol-insulin interaction was used to calculate the value of the energy parameter, ΔG , which was found to be $-4.8 \text{ kcal mol}^{-1}$. Interestingly, molecular docking experiments on eugenol-insulin interaction shows a similar value of CDocker energy ($-4.1 \text{ kcal mol}^{-1}$).

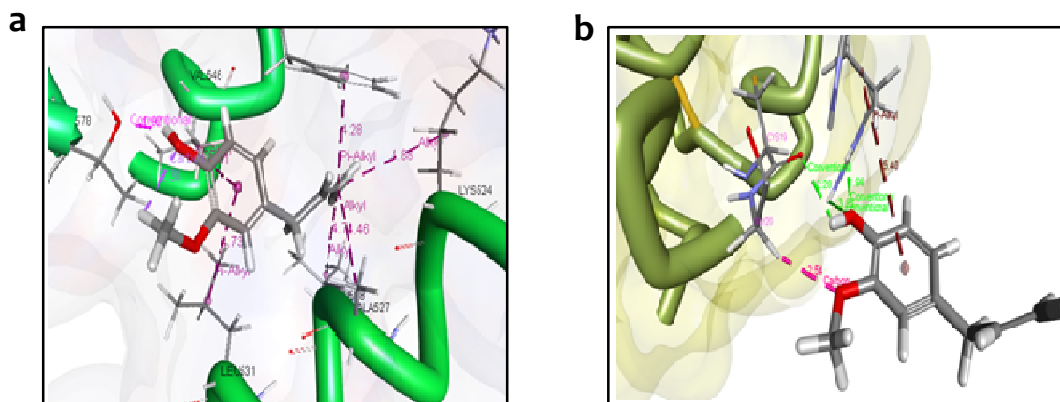


Figure 4.7 : (a) Docked complex of BSA (PDB ID: 4F5S) with eugenol represents seven interactions: one hydrogen bond (eugenol:H24 - A:THR578:OG1), three alkyl interactions (A:ALA527 - eugenol:C12, eugenol:C12 - A:LYS524, eugenol:C12 - A:LEU528), and three pi-alkyl interactions (A:PHE550 - eugenol:C12, eugenol - A:LEU531, eugenol - A:VAL546). (b) Docked complex of insulin (PDB ID: 4I5Z) with eugenol represents five interactions: four hydrogen bonds (B:ARG22:HE - eugenol:O2, B:ARG22:HH21 - eugenol:O2, eugenol:H24 - B:CYS19:O, and B:GLY20:HA1 - eugenol:O1) and one pi-alkyl interaction (eugenol - B:ARG22). The detailed information about the protein-ligand interactions is given in the Table 4.1 and 4.2.

Table 4.1 : Summary of BSA – Eugenol Interaction complex having –CDOCKER energy =13.9359 Kcal mol⁻¹, - CDOCKER interaction energy = 28.489 Kcal mol⁻¹

S. No.	Interacting residues	Bond Length (Å)	Interaction Type
1	Eugenol:H24 - A:THR578:OG1	1.91997	Conventional Hydrogen Bond
2	A:ALA527 - Eugenol:C12	4.45912	Alkyl
3	Eugenol:C12 - A:LYS524	4.88277	Alkyl
4	Eugenol:C12 - A:LEU528	4.70672	Alkyl
5	A:PHE550 - Eugenol:C12	4.28414	Pi-Alkyl
6	Eugenol - A:LEU531	4.73066	Pi-Alkyl
7	Eugenol - A:VAL546	5.00627	Pi-Alkyl

Table 4.2 : Summary of Insulin – Eugenol Interaction complex having –CDOCKER energy =4.03099 Kcal mol⁻¹, - CDOCKER interaction energy = 13.4501 Kcal mol⁻¹

S. No.	Interacting residues	Bond Length (Å)	Interaction Type
1	Eugenol- B:ARG22	5.39854	Pi-Alkyl
2	B:GLY20:HA1 - Eugenol:O1	2.54114	Carbon Hydrogen Bond
3	Eugenol:H24 - B:CYS19:O	2.28056	Conventional Hydrogen Bond
4	B:ARG22:HH21 - Eugenol:O2	3.05003	Conventional Hydrogen Bond
5	B:ARG22:HE - Eugenol:O2	1.96414	Conventional Hydrogen Bond

4.2 CAPSAICIN INHIBITS THE PROCESS OF COLLAGEN FIBRIL FORMATION

Capsaicin (8-methyl-*N*-vanillyl-6-nonenamide; Figure 4.11b) is a plant product which belongs to the class of capsaicinoids compounds. Capsaicin is widely used in foods and medicines because of its multiple health benefits, including its antihypertension, antitumorigenic and anti-inflammatory properties. Topical application of capsaicin is known to be effective against various pain complications that are associated with diseases such as diabetic neuropathy and osteoarthritis (Tandan, Lewis et al. 1992; Hempenstall, Nurmikko et al. 2005). In some previous reports it has been observed that inactivation of capsaicin-sensitive nerve fibers reduces pulmonary remodeling which takes place in collagen and elastic fibers and capsaicin treatment decreases the presence of collagen fibers in the vessels and lung tissues (Prado, Da Rocha et al. 2011). In some other investigations it has been reported that, capsaicin is capable to cross ECM barrier by penetrating through the skin (Fang, Fang et al. 2001) and collagen matrix (Ko, Diaz et al. 1998). Therefore there is a possibility that capsaicin is interacting with collagen assemblies while penetrating the skin. But reports on capsaicin-collagen interactions are very rare in literature. Hence, it is important to understand the effect of capsaicin on different biophysical properties of collagen, both in molecular form and higher order form.

Collagen is an integral component of ECM which is critical for both structural and functional property of many tissues in the body systems (Kielty and Grant 2003). During the process of collagen fibril formation, triple helical collagen monomers self-assembled into higher order supramolecular structures to form collagen fibers. The fibrillar collagen not only provides mechanical support but also helps in proper functioning of many tissues such as skin, tendon, and blood. But the excessive accumulation of fibrous collagen is sometimes associated to several pathologies. It is reported that, excess platelet aggregation mediated by fibrillar collagens can cause thrombosis which leads to myocardial infarction and stroke (Farndale, Sixma et al. 2004). Type VIII collagen is involved in atherosclerosis lesions and plaque formation (Plenz, Deng et al. 2003). When these plaques are ruptured, they form platelet thrombus which causes sudden heart attack if thrombus is formed in the coronary arteries or it may cause stroke if thrombus formation is in cerebral artery. Recently researches have verified the possibility of a link existing between fibrillar-collagen accumulation and tissue stiffness in hypertensive heart disease. Hence, it is important to find out inhibitors against collagen fibril formation, which may help both fundamental and applied research work on collagen.

Hence, this section of the thesis work is focused on the understanding of capsaicin-collagen relationship. The effect of capsaicin on different biophysical properties of type I collagen was studied, by using a combination of different biophysical and computational tools.

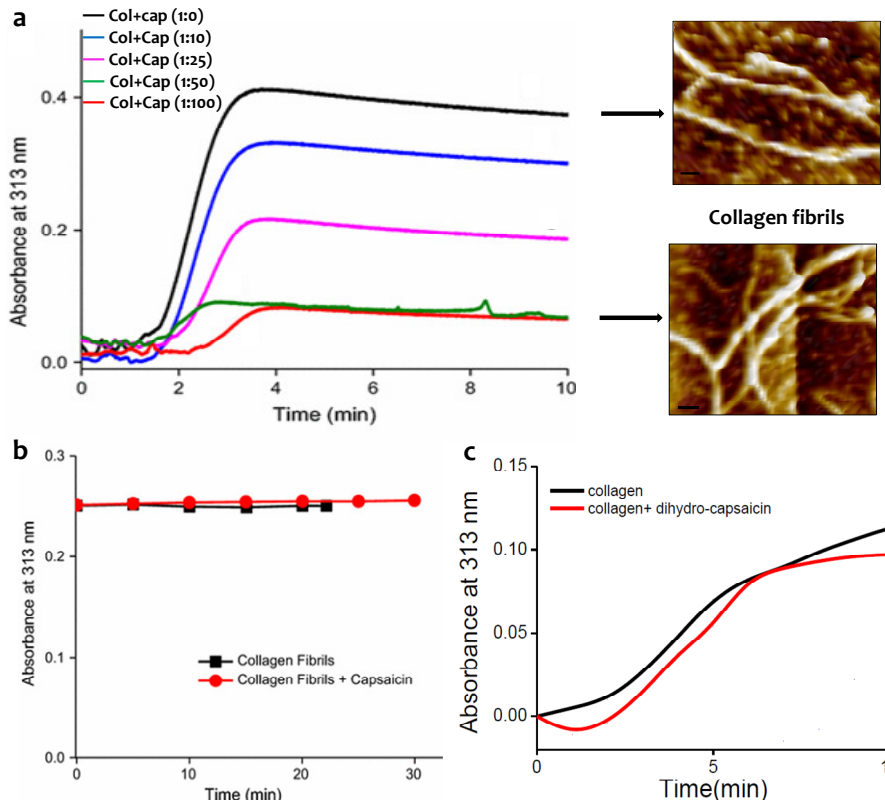


Figure 4.8 : Effect of capsaicin on type-1 collagen fibril formation and fibril dissociation. (a) Kinetics of collagen fibril formation was monitored in the presence and in the absence of capsaicin, at different molar ratios: Collagen alone (1:0, —), Collagen+capsaicin (1:10, —), Collagen+capsaicin (1:25, —), Collagen+capsaicin (1:50, —), and Collagen+capsaicin (1:100, —). Concentration of the collagen was kept at $\sim 1 \mu\text{M}$ in all the samples and the measurements were recorded in PBS buffer (pH 7.4) at 37°C . AFM images of final collagen fibrils in the absence and in the presence of capsaicin were also shown. Scale bar, $\sim 100 \text{ nm}$. (b) Effect of capsaicin on disassembly of collagen fibrils. Molar ratio of the collagen to capsaicin was 1:100 and the measurements were recorded at 25°C as a function of time. (c) Effect of dihydro-capsaicin on collagen fibril formation in PBS at 37°C . Collagen concentration was $\sim 0.1 \text{ mg/ml}$ and the molar ratio of collagen to dihydro-capsaicin was 1:100.

4.2.1 Effect of Capsaicin on Fibril Formation of Type I Collagen

Under *in vitro* conditions, when collagen monomers are incubated at temperature $\sim 37^\circ\text{C}$ and at pH 7.4, they readily form collagen fibrils. The process of collagen fibril formation can be monitored by recording the optical density of collagen sample as a function of time, at a wavelength of 313 nm (Mehta, Rao et al. 2014). In this work, to study collagen fibril formation, soluble collagen (at $\sim 1\ \mu\text{M}$ concentration) was incubated in PBS buffer at 37°C . Collagen sample without capsaicin showed a typical turbidity curve consisting of a lag phase, a growth phase and a plateau phase (Figure 4.8a, —). Hence, the obtained kinetics confirm the self-assembly of soluble collagen molecules into higher order fibrils. A gradual suppression in the formation of collagen fibril was observed with increasing concentration of capsaicin in the sample (Figure 4.8a). The turbidity data, as shown in Figure 4.8a, suggest that the lag time of the self-assembly process is not much delayed in the presence of capsaicin, however the extent of fibrils formed are substantially reduced. At 1:100 molar ratio of collagen to capsaicin, almost 90% reduction in the amount of fibrils formed was observed, with a slight delay in the lag time. Additionally, the AFM images of mature collagen fibrils, formed in the absence and in the presence of capsaicin, were analyzed and fibril obtained from both the reaction looks similar. Since lag time is not much affected, it is possible that suppression effect is achieved during the growth phase which involves inter-fibrillar association. It is also possible that interaction of capsaicin with the fibrillar form of collagen is more favorable than capsaicin-molecular collagen interaction. Another reason behind this inhibition effect could be promotion of fibril-disassembly in the presence of capsaicin. To understand the effect of capsaicin on fibril-disassembly, capsaicin was added to a suspension of mature collagen fibrils and the change in the optical density of the sample was measured as a function of time (Figure 4.8b). The obtained data clearly indicate that capsaicin did not promote disassembly of collagen fibrils (Figure 4.8b, ●).

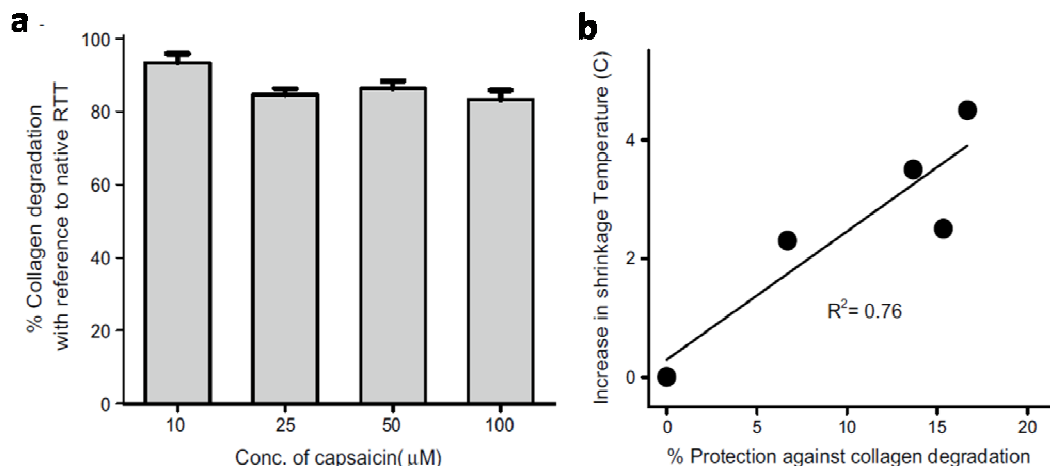


Figure 4.9 : (a) Protective effect of capsaicin against enzymatic degradation of rat tail tendons (RTT). The percentage of degradation of collagen tendons by collagenase enzyme was determined in the absence and in the presence of capsaicin (10 μM , 25 μM , 50 μM , and 100 μM). The collagen to collagenase ratio was maintained at 50:1 and the samples were incubated at 37°C for 96 hrs. All the measurements were repeated at least two times. (b) Correlation between the increase in shrinkage temperature and % protection against collagenase. R^2 for the linear regression fit is 0.76.

4.2.2 Effect of Capsaicin Against Enzymatic Degradation of Fibrillar Collagen

Further, to determine the binding properties of capsaicin with collagen fibers, collagenolytic degradation was performed on capsaicin treated rat tail tendons. The amount of hydroxyproline released from the collagenase treated RTT was measured to quantify the degradation of collagen fibrils in the presence of capsaicin. In this experiment, almost 99% of the native collagen fibers underwent degradation in the absence of capsaicin (Figure 4.9). Capsaicin treated RTT, however, showed resistance to collagenolytic hydrolysis (Figure 4.9a). As shown in

the Figure 4.9, about 20% less hydrolysis was observed in the presence of 100 μ M capsaicin. Since capsaicin treated collagen fibers were properly washed before their exposure to collagenase, interaction between collagenase and capsaicin seems to be less likely. Hence, this result suggests that capsaicin may have the ability to bind to the collagen fibers, and this binding may interfere with the catalytic action of the collagenase.

4.2.3 Hydrothermal Shrinkage of Tendons in the Presence of Capsaicin

To further understand capsaicin-tendon interaction the shrinkage temperature of RTT was measured in the presence of capsaicin. The hydrothermal shrinkage temperature measurement of RTT fibers is a direct evidence of thermal stability of ordered collagen fibers. Shrinkage temperature is the temperature at which the collagen tendon shrinks to one-third of its original length when heated in an aqueous medium. Various factors can influence such denaturation temperature of collagen fibers (21, 22). The obtained results of the shrinkage temperature of native tendons as well as capsaicin treated tendons (see Annexure A) are summarized in Table 4.3. The native collagen fibers exhibit a shrinkage temperature of $\sim 56^\circ\text{C}$, which is higher than the denaturation temperature of the collagen triple-helical molecules ($\sim 41^\circ\text{C}$). An increase in the shrinkage temperature of the collagen fibers was observed, which were pretreated with capsaicin (Table 4.3). The shrinkage temperature of RTT collagen fibers treated with 100 μ M of capsaicin was observed to be 60.5°C . Such an increase in the shrinkage temperature suggests a possible interaction between capsaicin and collagen fibers in tendon. This assumption is consistent with the data obtained from enzymatic degradation experiments on collagen fibers. A correlation between increase in shrinkage temperature and protection against collagenase is clearly evident from the plot shown in Figure 4.9b.

Table 4.3 : Hydrothermal stability of rat tail tendons (RTT) treated with different concentrations of capsaicin

Concentration of capsaicin (mM)	Shrinkage temperature ($^\circ\text{C}$)
0	56.0 ± 0.8
1	57.0 ± 0.8
10	58.3 ± 0.5
20	58.5 ± 0.6
50	59.5 ± 0.5
100	60.5 ± 0.5

4.2.4 Effect of Capsaicin on the Conformational Stability of Collagen Triple-helix

Since the shrinkage temperature of collagen tendons was found increased in the presence of capsaicin (Table 4.3), as a next step, the effect of capsaicin on the thermal stability of molecular collagen was examined. The molecular structure of collagen is a triple helix and it has a characteristic CD signal at 222 nm. Hence, the CD spectra of collagen in the presence and in the absence of capsaicin were monitored, for a range of 250-210 nm (Figure 4.10a). From the obtained results it was clear that in the presence of capsaicin, collagen molecules retained their inherent triple-helical conformation (a positive peak at ~ 222 nm). Next, thermal unfolding of collagen triple-helical molecules was monitored by the change in the CD signal at 222 nm. The thermal unfolding curves suggest a slight increase in the T_m values of collagen molecule in the presence of capsaicin (Figure 4.10b). These results suggest that in the presence of capsaicin the conformational stability of triple-helical collagen molecule remains almost unaltered, whereas the thermal stability of collagen fibers is substantially increased (Table 4.3).

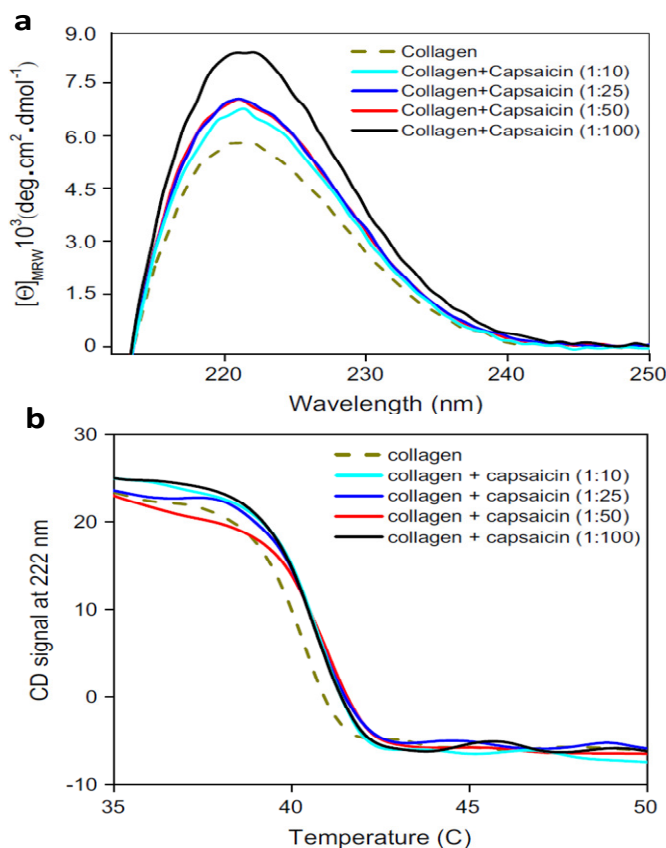


Figure 4.10 : CD spectroscopic studies of collagen-capsaicin interactions. (a) CD spectra of molecular collagen in the presence and in the absence of capsaicin, recorded at different molar ratios. (b) Thermal unfolding of type-1 collagen was measured in the presence and in the absence of capsaicin. The change in the CD signal at 222 nm for the triple-helix was monitored as the temperature of the sample was increased from 20 to 60°C at a rate of 1°C min⁻¹. All the CD scans shown here were average values of three accumulations.

4.2.5 Computational Docking Studies of Capsaicin with Selected Triple-Helical Collagen Model Peptides

Since the above experimental results indicated possible interaction between capsaicin and collagen, it is further important to understand the interaction that takes place between them at molecular level. To address this issue, molecular docking studies were conducted using Discovery Studio 4.0. From the docking results, it was observed that capsaicin was docked around specific triplets in each of the model collagen peptides (PDB id's: 1CAG, 1Q7D, 2DRT and 1QSU) (Figure 4.11, and 4.13 to 4.16). The data retrieved from 1CAG and capsaicin binding studies indicate that capsaicin binds with Gly-Pro-Hyp triplet (Figure 4.11). Capsaicin formed 3 hydrogen bonds (between HA of Pro37 and O2 of capsaicin, =O of Gly36 and H45 of capsaicin and =O of Gly36 and H46 of capsaicin) and participated in a mixed pi/alkyl hydrophobic interaction (between electron clouds of benzene subunit of capsaicin and cyclo-pentane subunit of Pro37). The CDocker energy score was -4.977 and interaction energy score was -17.404 which indicate a stable interaction between capsaicin and collagen. To confirm the role of functional groups of capsaicin that were identified to be involved in making interactions with Gly-Pro-Hyp triplets, 10 capsaicin decoys (See Annexure A) were identified and were subjected to docking studies using the same procedure. Except for one molecule (ZINC35317807, Figure 4.12), none showed any interaction with Gly-Pro-Hyp regions.

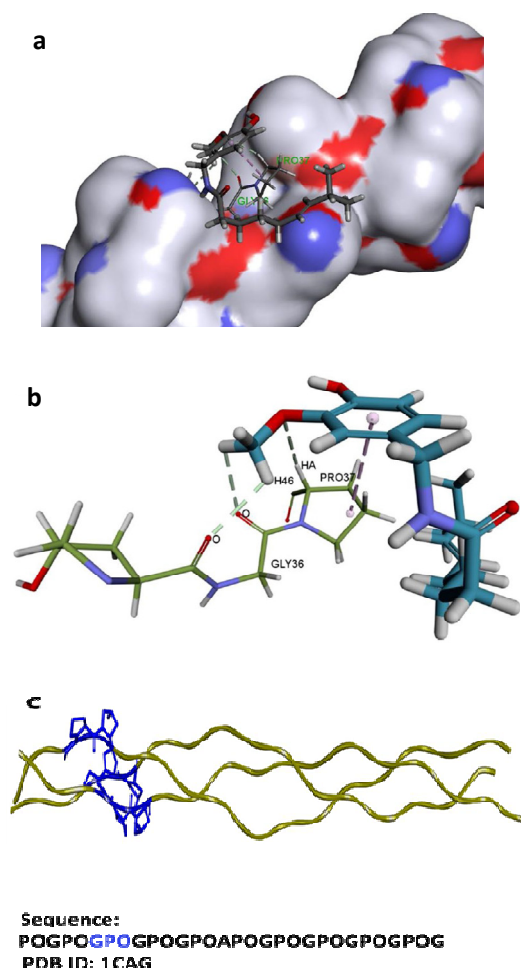


Figure 4.11 : Docking of capsaicin with Gly-Pro-Hyp triplet of the triple-helical collagen like peptide (PDB ID: 1CAG). (a) Capsaicin docked with the collagen triple helix, the triple-helix surface of which is rendered as its electron-density map. (b) Molecular interaction of capsaicin with the collagen triple helix. Hydrogen bonds are shown with *gray dotted lines*, whereas the electrostatic interaction is shown with a *light purple dashed line*. The docking studies were performed by the use of Discovery Studio 4.0 (see Annexure A). (c) Capsaicin docking region was highlighted in the collagen triple helical peptide.

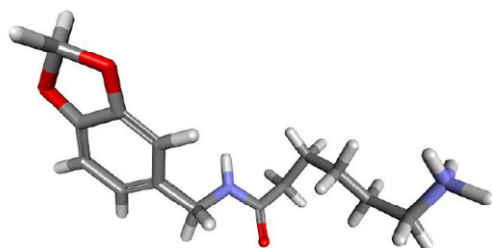
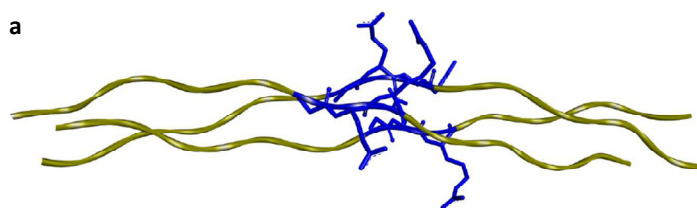


Figure 4.12 : Representing a decoy of capsaicin; **ZINC35317807**, that showed interaction with GPO regions of collagen peptide (PDB ID: 1CAG) . This study was performed to confirm the role of functional groups of capsaicin that were identified to be involved in making interactions with GPO triplets of 1CAG peptide, 10 capsaicin decoys (See Annexure A) were identified by the use of ZINC database.



Sequence: XGPOGPOGFO**GER**GPOGPOGPOX
 PDB ID: 1Q7D

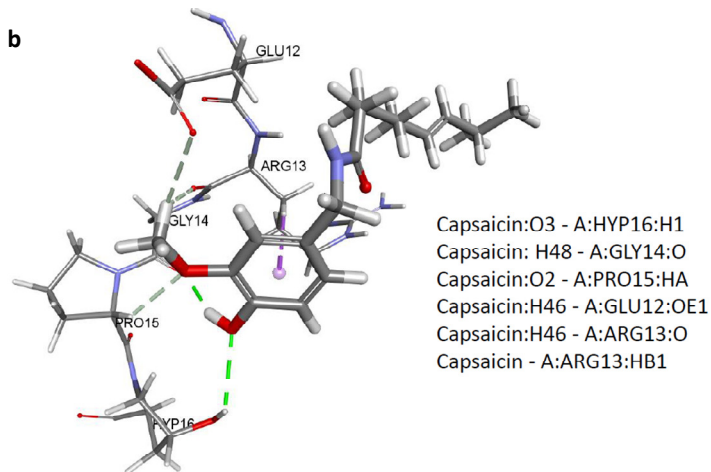
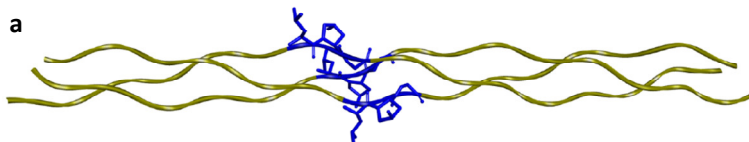


Figure 4.13 : Docking of capsaicin with GER triplet was carried out using a triple-helical collagen like peptide (PDB ID: 1Q7D). (a) Capsaicin docking region was highlighted in the collagen triple helical peptide. (b) Interaction of capsaicin with the triple helix. Hydrogen bonds are shown with *gray dotted lines*, whereas the summary of H-bond interactions taking place was also mentioned.



Sequence: GPOGPOGPOGPOG**LOG**POGPOGPOGPOG
 PDB ID: 2DRT

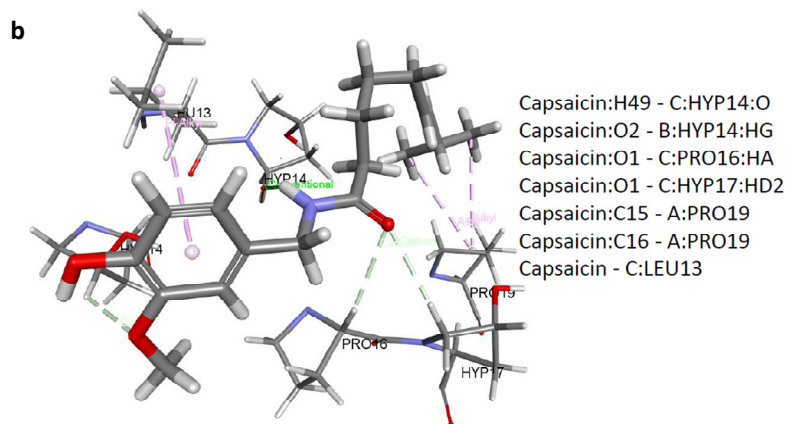


Figure 4.14 : Docking of capsaicin with LOG triplet was carried out using a triple-helical collagen like peptide (PDB ID: 2DRT). (a) Capsaicin docking region was highlighted in the collagen triple helical peptide. (b) Interaction of capsaicin with the triple helix. Hydrogen bonds are shown with *gray dotted lines*, whereas the summary of H-bond interactions taking place was also mentioned.

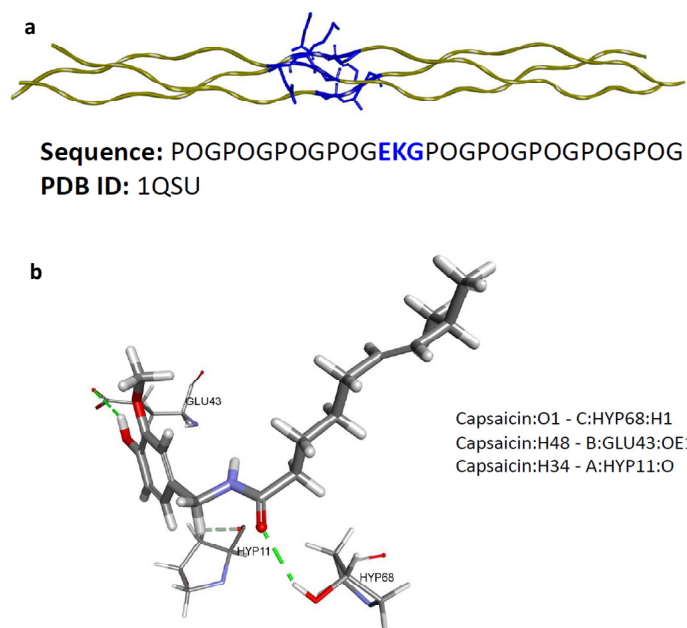


Figure 4.15 : Docking of capsaicin with KEG triplet was carried out using a triple-helical collagen like peptide (PDB ID: 1QSU). (a) Capsaicin docking region was highlighted in the collagen triple helical peptide. (b) Interaction of capsaicin with the triple helix. Hydrogen bonds are shown with *gray dotted lines*, whereas the summary of H-bond interactions taking place was also mentioned.

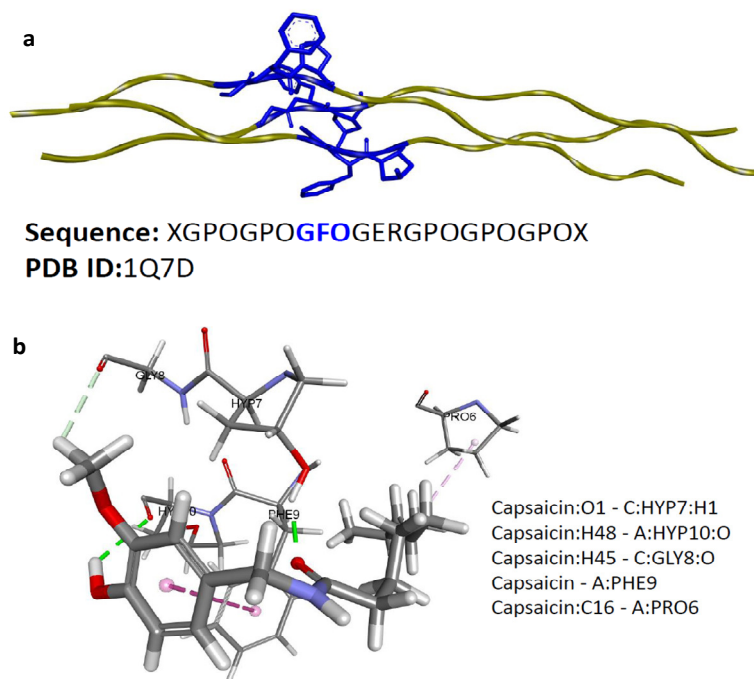


Figure 4.16 : Docking of capsaicin with GFO triplet was carried out using a triple-helical collagen like peptide (PDB ID: 1Q7D). (a) Capsaicin docking region was highlighted in the collagen triple helical peptide. (b) Interaction of capsaicin with the triple helix. Hydrogen bonds are shown with *gray dotted lines*, whereas the summary of H-bond interactions taking place was also mentioned.

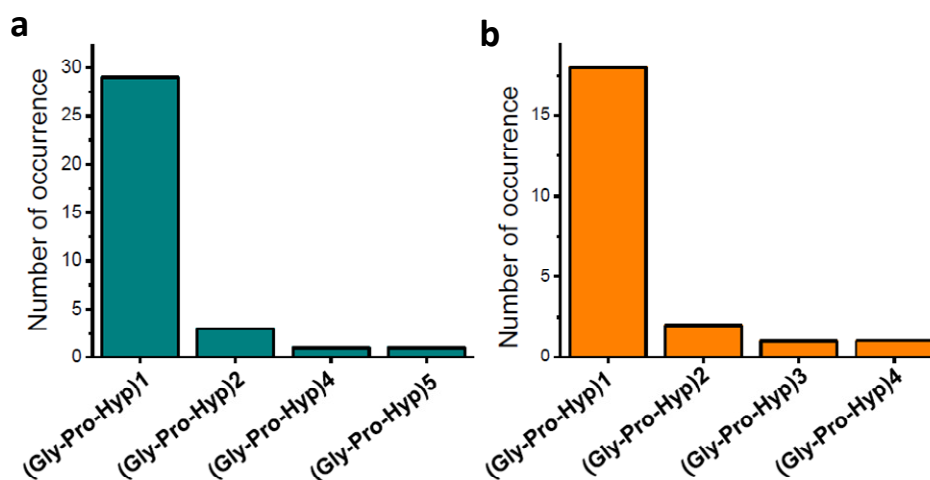


Figure 4.17 : Analysis of (Gly-Pro-Hyp) repeats present in the sequence of type I collagen: (a) α -1 chain of collagen; (b) α -2 chain of collagen.. In type I rat collagen there are two α -1 chains (NCBI Accession ID: AAI33729 & UniProt ID: P02454) and one α -2 chain (NCBI Accession ID AAD41775 & UniProt ID: P02466, Organism- *Rattus norvegicus*).

Further, other docking studies were also conducted between capsaicin and selected triple-helical model peptides containing sequences that are found in type I collagen. The details of the docking results have been summarized in the Figures 4.13 to 4.16. As observed from the interactions, capsaicin could potentially bind to “GFOGER”, “EKG”, and “GLO” sequences within the triple helical conformation.

4.3 DISCUSSION

In the first study of this chapter, it was observed that eugenol has the ability to inhibit or to interfere with the amyloid formation of insulin and serum albumin. It was also found that eugenol can prevent rapid coaggregation of [lysozyme+ insulin+serum albumin] sample. One of the factors that trigger the onset of temperature induced amyloid formation is believed to be the increase in the population of aggregation prone protein intermediate (I) species (Kar and Kishore 2007; Chiti and Dobson 2009). Besides that, these intermediate species, with exposed hydrophobic side chains, are known to promote intermolecular interactions leading to formation of amyloids. Because protein-ligand interactions play a key role in preventing protein aggregation (Soldi, Plakoutsi et al. 2006), it is possible that the occurrence of eugenol-protein interactions may stabilize the native conformations to shift the equilibrium of $N \rightleftharpoons I$ toward the left, thus reducing the population of the aggregation-prone intermediate species. Soldi et al. have suggested that the stabilization of native proteins due to ligand binding is an important factor for prevention of amyloid formation and such inhibition effect should occur independent of the aggregation pathways (Soldi, Plakoutsi et al. 2006). The ability of the ligand molecule to bind to preformed fibrillar species during amyloid formation can also be considered as another critical factor behind the inhibition mechanism. During the onset of an aggregation process, if any ligand has the potential to bind to the fibrillar species, the occurrence of such binding may prevent further addition of monomers. In turn, such binding would ultimately suppress the progress of the aggregation reaction. In addition to its affinity for protein monomers, eugenol seems to have the potential for binding to the aggregated species. The molecular docking studies have indicated the possibility of formation of stable insulin-eugenol and BSA-eugenol complexes. The interaction of eugenol with BSA has already been reported by Fujisawa et al. (Fujisawa and Masuhara 1981). The data obtained from CD and ThT measurements largely agree to this mechanism of stabilization of monomers as well as on pathway oligomers because native like structures were retained in the presence of eugenol during the process of amyloid

formation (Figure 4.5a and 4.5b). Eugenol has an interesting structure in which an aromatic moiety is linked to a hydrocarbon chain, a hydroxyl group and a methoxy group. Both methoxy and hydroxyl groups are known to be vital for eugenol's antioxidant property (Gulcin 2011). Studies have suggested that eugenol is capable of interacting with protein domains through multiple binding poses (Pechlaner and Oostenbrink 2015). Docking studies display the involvement of -OH and -O-CH₃ groups in hydrogen bonding interactions and the aromatic moiety is observed to be engaged with CH- π interactions. Further, the hydrocarbon chain of eugenol shows its involvement in CH- π interactions with aromatic side chains of the interacting protein. Therefore, it is believed that all these interactions are critical for the eugenol molecule to inhibit the process of amyloid formation.

In this study, strong inhibition of collagen fibril formation was observed when the concentration of capsaicin was increased to ~100 fold higher than the concentration of collagen. The type-I collagen triple helix is a hetero trimer which contains two α 1 chains and one α 2 chain. Each α chain contains approximately ~1,000 amino acids. It is possible that the whole sequence of both the α 1 and α 2 chains may have multiple sites facilitating binding of capsaicin. Computational docking studies suggest that Gly and Pro participate in collagen-capsaicin interactions. Further studies of docking of capsaicin with other collagen peptides (Figures 4.13 to 4.16) also indicated its interaction with the "GFOGER", "EKG", and "GLO" regions. Sequence analysis of type-I rat collagen showed that the α 1 chain contains 44 Gly-Pro-Hyp regions and 127 Gly-Pro sites. Similarly, the α 2 chain contains 29 Gly-Pro-Hyp regions and 116 Gly-Pro sites (Figure 4.17). This could be one reason for the requirement of such a high molar ratio of capsaicin to collagen (100:1) to prevent collagen fibril formation. It was believed that both hydrophobic and hydrophilic interactions mediated by capsaicin may directly link to the mechanism of suppression of collagen fibril formation. Inhibition of fibril formation by capsaicin suggests that capsaicin may interfere with aggregation of collagen molecules as a result of its interaction with monomolecular collagen. The interactions that occur between capsaicin and collagen in the monomolecular and fibrillar forms might not have the same effect. Although capsaicin does not alter the thermal stability of triple-helical collagen molecules, it increases the shrinkage temperature of tendons and protects them from enzymatic degradation. Collagen forms a highly ordered, quarter-staggered arrangement in which collagen triple helical molecules are fixed at defined dimensions in 3D space. It is, therefore, possible that capsaicin can participate in multipoint interactions between collagen molecules (in the fibrillar form), which may enhance the stability of collagen fibers.

4.4 CONCLUSION

The eugenol molecule seems to be a very promising candidate for prevention of protein amyloid formation of proteins. Stabilization of the native protein structures and the intermediate oligomeric species seems to be crucial for the inhibition of protein aggregation in the presence of eugenol. Further experiments are certainly required to confirm this inhibition effect on other amyloidogenic proteins and peptides. However, for therapeutics against medical severities associated with insulin aggregation, the design of eugenol based drugs could be beneficial.

The present study on capsaicin and collagen interaction demonstrates the potential of capsaicin to suppress collagen fibril formation. Accumulation of collagen is one of the main causes for the onset of many lethal complications such as fibrosis and atherosclerosis. Therefore, a straightforward approach to target collagen fibril formation could be critical for treating diseases associated with excess collagen accumulation. Utilization of this unique property of capsaicin may help us in the development of potential drugs against diseases linked to excess collagen fibrillogenesis.